BAMS Article

Routine Climate Monitoring in the State of Hawai'i: Establishment of State Climate Divisions

Xiao Luo,[a,d,e] Abby G. Frazier,[a,b,c] Henry F. Diaz,[c] Ryan Longman,[a,f] and Thomas W. Giambelluca[a,c]

KEYWORDS:
Tropics;
Climate change;
Climate classification/regimes;
Climate variability;
Clustering

ABSTRACT: The Hawaiian Islands have some of the most spatially diverse rainfall patterns on Earth, affected by prevailing trade winds, midlatitude disturbances, tropical cyclones, and complex island topography. However, it is the only state in the United States that does not have assigned climate divisions (boundaries defining climatically homogeneous areas), which excludes it from many national climate analyses. This study establishes, for the first time, official climate divisions for the state of Hawai'i using cluster analysis applied to monthly gridded rainfall data from 1990 to 2019. Twelve climate divisions have been identified: two divisions were found each for the islands of Kaua'i (Leeward Kaua'i and Windward Kaua'i), O'ahu (Waianae and Ko'olau), and Maui County (Leeward Maui Nui and Windward Maui Nui), and six divisions were identified for Hawai'i Island (Leeward Kohala, Windward Kohala, Kona, Hawai'i Mauka, Ka'u, and Hilo). The climate divisions were validated using a statewide area-weighted division-average rainfall index which successfully captured the annual cycle and interannual rainfall variations in the statewide average rainfall series. Distinct rainfall seasonality features and interannual/decadal variability are found among the different divisions; Leeward Maui Nui, Leeward Kaua'i, Kona, and Hawai'i Mauka displayed the most significant rainfall seasonality. The western Hawai'i Island divisions show the most significant long-term decreasing trends in annual rainfall during the past 100 years (ranging from −2.5% to −5.0% per decade). With these climate divisions now available, Hawai'i will have access to numerous operational climate analyses that will greatly improve climatic research, monitoring, education, and outreach, as well as forecasting applications.

SIGNIFICANCE STATEMENT: The Hawaiian Islands have some of the most spatially diverse climate patterns on Earth, but it is the only state in the United States that does not have assigned climate divisions, which excludes it from many national climate analyses. This paper establishes official climate divisions for the state of Hawai'i, filling an incredibly important gap in the National Oceanic and Atmospheric Administration (NOAA)'s national coverage, moving toward better data equity and coverage outside the contiguous United States. Distinct rainfall seasonality features and interannual/decadal variability are revealed and compared among the different divisions. With these climate divisions now available, Hawai'i will have access to numerous operational climate analyses that will greatly improve climatic research, monitoring, education, and outreach, as well as forecasting applications.

DOI:10.1175/BAMS-D-23-0236.1
Corresponding author: Xiao Luo, luoxiao.rf@gmail.com
Supplemental information related to this paper is available at the Journals Online website: https://doi.org/10.1175/BAMS-D-23-0236.s1.

Manuscript received 4 September 2023, in final form 7 March 2024, accepted 11 March 2024

AFFILIATIONS: [a] Water Resources Research Center, University of Hawai'i at Mānoa, Honolulu, Hawaii; [b] Graduate School of Geography, Clark University, Worcester, Massachusetts; [c] Department of Geography and Environment, University of Hawai'i at Mānoa, Honolulu, Hawaii; [d] School of Ocean Earth Science and Technology, Department of Atmospheric Sciences and International Pacific Research Center, University of Hawai'i at Mānoa, Honolulu, Hawaii; [e] Lynker at NOAA/NWS/NCEP/EMC, College Park, Maryland; [f] East-West Center, Research Program, Honolulu, Hawaii

1. Introduction

The Hawaiian Islands have some of the most highly spatially diverse climate patterns on Earth. The complex island topography (0–4205 m), persistent trade winds, thermal effects, and the presence of an atmospheric inversion layer called the trade wind inversion (TWI) produce extremely steep climate gradients, with mean annual rainfall ranging from 204 to 10 271 mm (Fig. 1; Giambelluca et al. 2013). Many recent efforts have attempted to map these climate patterns, producing high-resolution gridded datasets of mean monthly rainfall (Giambelluca et al. 2013) and time series of monthly and daily rainfall starting in 1920 and 1990, respectively (Frazier et al. 2016; Longman et al. 2019; Lucas et al. 2022). Gridded monthly and daily temperature datasets are also available (Kodama et al. 2024), and all gridded products have been recently made available in near–real time on the Hawai'i Climate Data Portal (Longman et al. 2024). These products have been widely used for numerous studies in Hawai'i [e.g., studies of streamflow (Clilverd et al. 2019); ecosystems (Barbosa and Asner 2017; Frauendorf et al. 2019; Frazier et al. 2022); and agriculture (Adhikari et al. 2022)]; however, the lack of official climate divisions still excludes the state from many other national-scale analyses (e.g., Vose et al. 2014).

Rainfall in Hawai'i exhibits a number of extremes that include some of the wettest locations on Earth and short-term extreme events that rival national extreme values. For example, the island of Kaua'i set the U.S. 24-h rainfall record in April 2018, receiving 49.7 in. (1262 mm; Corrigan and Businger 2022). Extreme droughts also regularly affect the state with severe impacts on agriculture, ecosystems, and water supplies (Frazier et al. 2019, 2022; Eischeid et al. 2022). Rainfall in Hawai'i is also strongly modulated by large-scale modes of natural variability, like El Niño–Southern Oscillation (ENSO) and the

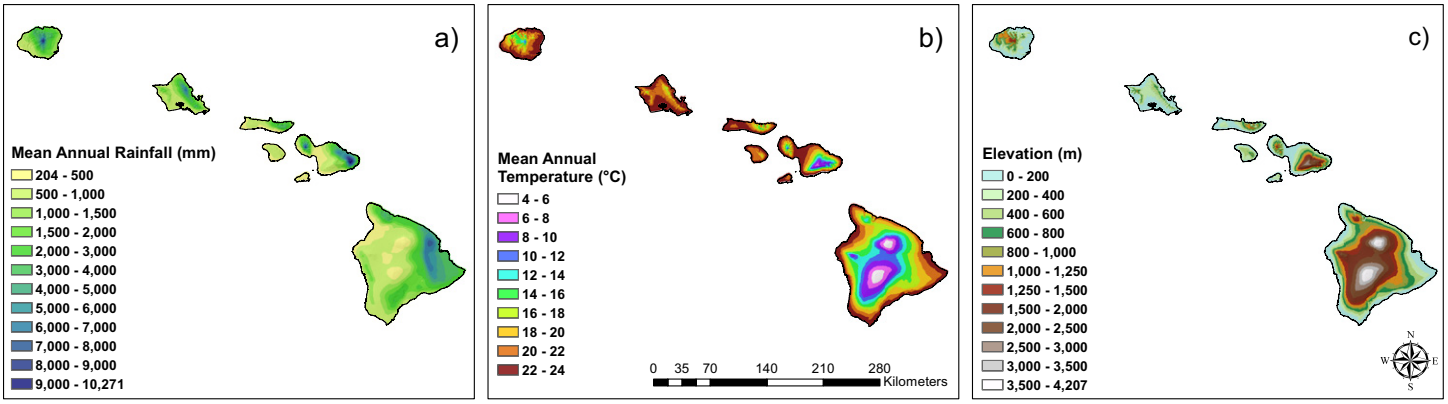

Fig. 1. (a) Mean annual rainfall (1978–2007; Giambelluca et al. 2013); (b) mean annual temperature (Giambelluca et al. 2014); and (c) elevation for the state of Hawai'i.

Pacific decadal oscillation (PDO) (e.g., Chu and Chen 2005; Frazier et al. 2018); ENSO, in particular, is known to be an important driver of drought in Hawai'i (Frazier et al. 2022). While statewide rainfall has been declining, trends are heterogeneous, with stronger drying in some leeward (western) areas of the state (Frazier and Giambelluca 2017). Secular surface temperature changes in Hawai'i indicate significant warming in the past several decades as well as an amplification of the warming signal with elevation (McKenzie et al. 2019)—although the vertical distribution of temperature trends exhibits some unusual features, likely related to drying of the lower atmosphere and increasing cloud base heights (Kagawa-Viviani and Giambelluca 2020). Since most gridded extreme climate products in the United States rely on climate division datasets, such as the gridded standardized precipitation index (SPI; Durre et al. 2022), these are only available for the contiguous United States (CONUS). Hawai'i, therefore, has had to rely on local efforts to calculate similar indices (e.g., gridded SPI for Hawai'i; Lucas et al. 2020).

Basic climate summaries and historical climate analyses produced by the National Oceanic and Atmospheric Administration (NOAA)'s National Centers for Environmental Information (NCEI) do not include the state of Hawai'i, largely because Hawai'i is the only state that does not have assigned climate divisions. The CONUS is separated into 344 climate divisions (Guttman and Quayle 1996), while Alaska has an additional 13 divisions which were added to the national dataset in 2015 (Bieniek et al. 2012). In 1909, the CONUS was divided into 12 climatological districts. Later, 106 climate divisions were established in 1912; however, the boundaries were primarily based on economical mailing practicality rather than climatically homogenous regions (Guttman and Quayle 1996). In the 1950s, the network was expanded to 344 climate divisions considering geography, drainage basins, river districts, and forecast areas of responsibility (Guttman and Quayle 1996). Climatic time series within each division were calculated by averaging the station values within each division. In 2014, the NCEI Monitoring Branch transitioned to a new method of calculating divisional values using a 5-km grid-based calculation. NCEI products that use the climate divisions include "Climate at a Glance," "Monthly National Climate Reports," "National Temperature Index," "Weekly Divisional Products," "Weekly Palmer Drought Indices," and others (see https://www.ncei.noaa.gov/access/monitoring/products/).

Given the extreme climatic variations and the severe risks that Hawai'i faces with ongoing climate change (e.g., Keener et al. 2018; Frazier et al. 2023), there is a critical need to establish official climate divisions for Hawai'i and improve national climate services. The exclusion of Hawai'i and other U.S. territories from national data collection efforts perpetuates historical social injustices (Frazier et al. 2023; Méndez-Lazaro et al. 2023). These data inequities can hinder timely data-driven decision-making and climate adaptation planning, funding, and implementation in frontline, socioeconomically disadvantaged, and Indigenous communities (Keener et al. 2022). It is imperative that the scientific community work together to fill these data gaps to better understand climate risks and inform responses (Basile et al. 2024).

Our objectives are to develop the analytical approach to produce climate divisions for the state of Hawai'i with regional groupings analogous to the CONUS climate division records. Given the strong spatial climate gradients in Hawai'i, a careful analysis is needed to develop appropriate climate divisions that characterize the state's spatial and temporal variabilities, to better understand the impact of climate variability and change, and to be able to include the state within NCEI's suite of state and national climate products. The development of climate divisions for the state of Hawai'i will support the development of a robust monitoring and forecasting framework, enhancing seasonal forecasting at the NOAA National Weather Service (NWS) and Climate Prediction Center (CPC) (e.g., providing context and rationale for the refinement of NWS/CPC outlooks), as well as monitoring through NCEI.

2. Data and methods

a. Data. Monthly rainfall data, both gridded data and rain gauge station data, from 1990 to 2019 were used in this study (Lucas et al. 2022). The rain gauge network is generally denser over Oʻahu and central Maui than in other areas. Over Kauaʻi and Hawaiʻi Islands, most stations are found in coastal areas, while fewer stations are located in high-elevation areas. The gridded monthly rainfall has a spatial resolution of 250 m and spans seven of the eight main Hawaiian Islands (from 18.849°N, 154.668°W to 22.269°N, 159.816°W). The island of Niʻihau is excluded due to lack of data. For this study, the islands in Maui County (Maui, Molokaʻi, Lānaʻi, and Kahoʻolawe) are referred to as "Maui Nui." Monthly rainfall grids were created using an optimized geostatistical kriging approach to interpolate relative rainfall anomalies which are then combined with long-term means to develop the climatologically aided gridded estimates (Lucas et al. 2022). Optimization of the kriging algorithm consists of 1) determining an offset (constant) to use when log-transforming data, 2) quality controlling data prior to interpolation, 3) using machine learning to detect erroneous maps, and 4) identifying the most appropriate parameterization scheme for fitting the model used in the interpolation. The station data were partially gap filled to improve the spatial coverage of the dataset, resulting in a dataset of 618 stations available from 1990 to 2019 (see the distribution of stations in Fig. 2). For a complete description of quality control and gap-filling steps, please see Longman et al. (2020) and Lucas et al. (2022). The rainfall data (both gridded and station data) are accessible online through the Hawaiʻi Climate Data Portal, http://www.hawaii.edu/climate-data-portal (Longman et al. 2024).

The monthly surface temperature data from 1990 to 2019 are also available on the Hawaiʻi Climate Data Portal (Kodama et al. 2024; Longman et al. 2024). This study included both gridded data (250 m spatial resolution) and station data. A total of 216 stations were used to create gridded temperature data from 1990 to 2019 at a 250-m spatial resolution using a piecewise linear regression model with elevation as the sole predictor (Kodama et al. 2024).

The oceanic Niño index (ONI) was calculated based on a merged sea surface temperature (SST) dataset which was made by averaging two monthly mean SST datasets from 1920 to 2019: the Hadley Center Sea Ice and Sea Surface Temperature dataset version 1 (HadISST1) (Rayner et al. 2003) and Extended Reconstructed SST (ERSST) V5 global SST monthly dataset (Huang et al. 2017). The ONI is calculated by averaging the SSTs over the Niño-3.4 region from October to the next February for each year. The monthly PDO index (Mantua et al. 1997) from NOAA NCEI (https://www.ncdc.noaa.gov/teleconnections/pdo/) based on ERSST V5 is used in this study. These indices were correlated with wet season and dry season Hawaiian rainfall from 1990 to 2019 to detect potential signals modulating rainfall over different divisions.

b. Methods. The *k*-means cluster analysis (Wilks 2011) was used to distinguish different divisions in Hawaiʻi. The *k*-means cluster analysis uses squared correlation distance to measure the "similarity" between each cluster member and the corresponding cluster centroid. The monthly gridded rainfall data from 1990 to 2019 were used for cluster analysis (Lucas et al. 2022). To determine the optimal number of clusters, analyses with 8–16 clusters were examined by local experts (including local climatologists with over 40 years of experience studying Hawaiʻi's climate patterns and local National Weather Service and NOAA NCEI staff). The sum of squared distances between clusters was examined to determine if a clear "elbow point" emerged. The expert team considered many factors, including known climate drivers (e.g., trade wind–driven orographic patterns) and local factors (e.g., onshore winds in the Kona region compared to other leeward locations; Giambelluca et al. 2013). To improve computing efficiency, the 250-m resolution grids were first resampled to 2 km and then cluster analysis was applied to the 2-km resolution monthly rainfall data. To test the representativeness

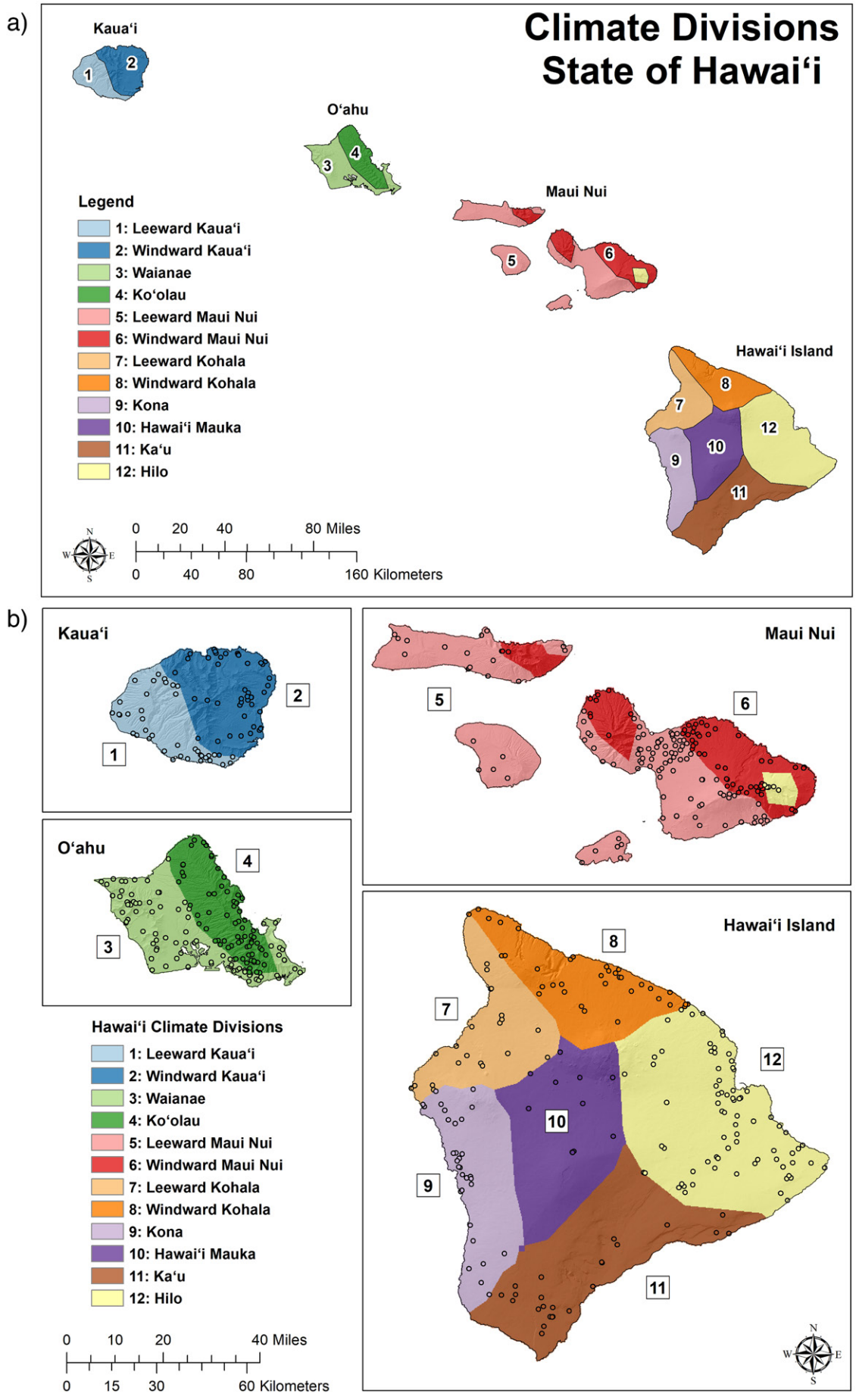

FIG. 2. (a) The 12 climate divisions for the state of Hawai'i. A list of division names has been provided in Table 1. (b) The stations located within each division; the scale of the islands is the same in each subpanel.

of the rainfall-based climate divisions, the cluster analysis was rerun using 1) surface temperature data and 2) a merged rainfall and surface temperature dataset.

To evaluate whether the climate divisions were representative and sufficiently capturing the rainfall variability, four statewide mean rainfall indices were calculated and compared: the spatial average of the statewide gridded rainfall (GRID), the average of rainfall over all 618 stations (STN-AVG), the average of rainfall at all the stations within each of the divisions and an average of the divisions (DIV-AVG), and an area-weighted average of the station-based division averages, using the area of each division as the weight (DIV-WGT).

Long-term monthly rainfall variability was examined within each division from 1920 to 2019 using a merged gridded rainfall dataset. Monthly gridded rainfall data from 1920 to 2012 (Frazier et al. 2016) were merged with monthly gridded rainfall from 1990 to 2019 (Lucas et al. 2022) by taking the arithmetic mean of the two datasets for the overlapped years (1990–2012).

To quantify the seasonality strength, we used the seasonality index (SI) (Walsh and Lawler 1981), estimated using the following equation [Eq. (1)]:

$$\mathrm{SI} = \frac{1}{R}\sum_{n=1}^{n=12}\left|R_n - \frac{R}{12}\right|, \tag{1}$$

and the ratio of the highest monthly rainfall to the lowest monthly rainfall (R_{hl}) (Getz and Nilsson 2004) [Eq. (2)],

$$R_{\mathrm{hl}} = \frac{R_{\max}}{R_{\min}}. \tag{2}$$

In these equations, $R_{\max}$ and $R_{\min}$ denote the climatological maximum and minimum monthly rainfall, respectively. The R is the total climatological annual precipitation and R_n is the climatological monthly precipitation for month n. The R_{hl} and SI were calculated for each of the divisional indices. Higher values of R_{hl} indicate stronger seasonality. Different climate categories based on rainfall seasonality can be determined using the SI values. For instance, a range of 0.20–0.39 indicates precipitation dispersed across the year, but with a distinct wetter season, whereas the range of 0.40–0.59 corresponds to a somewhat seasonal pattern with a shorter dry season (Walsh and Lawler 1981).

3. Results and discussion

a. Climate division boundaries. Based on a combination of cluster analysis on monthly rainfall and local expert knowledge, we have identified 12 climate divisions (divisions here forward) for the state of Hawai‘i (Fig. 2). The sum of squared distances between clusters did not exhibit a clear elbow point; therefore, local expert knowledge provided critical background information and guidance in selecting the number of divisions. We numbered the divisions from north to south and from west to east, as seen in Fig. 2. Each division was given a specific name related to its local geography as shown in Table 1.

The results show that Kaua‘i, O‘ahu, and Maui Nui have two divisions each. Divisions on Kaua‘i and O‘ahu have continuous spatial distributions, while divisions on Maui Nui span multiple islands. Leeward Maui Nui includes Maui, Moloka‘i, Lāna‘i, and Kaho‘olawe. Windward Maui Nui includes a portion of the windward area of Moloka‘i. Hawai‘i Island is divided into six divisions, with Hawai‘i Mauka in the center surrounded by five coastal divisions. The Hilo Division covers a large area on the eastern (windward) side of Hawai‘i Island as well as a small area of windward Maui. Leeward Kohala and Windward Kohala are located in the north and Ka‘u Division in the southern part of Hawai‘i Island. The Kona Division is an area with distinct climate variability features, notably, its unique annual cycle with peak rainfall in summer months (Giambelluca et al. 2013).

Table 1. Names of each climate division and their area (km^2), percent of the statewide area, and the number of rain gauge stations within each division as of 2019.

Division number	Division name	Area (km^2)	Percent area (%)	Number of stations
1	Leeward Kaua'i	591.2	4	37
2	Windward Kaua'i	871.6	5	48
3	Waianae	941.1	6	84
4	Ko'olau	661.0	4	74
5	Leeward Maui Nui	2030.8	12	103
6	Windward Maui Nui	990.5	6	11
7	Leeward Kohala	1173.1	7	24
8	Windward Kohala	1213.6	7	36
9	Kona	1303.6	8	30
10	Hawai'i Mauka	1747.1	11	9
11	Ka'u	2069.5	13	26
12	Hilo	2851.6	17	81

Cluster analysis was also applied to temperature data and a rainfall–temperature merged dataset. The results showed that most of the divisions based on temperature data were elevation and latitude driven, and many regions were in elevational band shapes along the highest peaks of Mauna Kea and Mauna Loa in Hawai'i Island (figure not shown). The cluster analysis results using the merged temperature and rainfall data show that rainfall variability plays a dominant role in determining the division boundaries (figure not shown). The results are similar to those derived from the rainfall-based analysis results, suggesting that there is limited diversity in the temperature variability. Therefore, rainfall was determined to be the most appropriate variable for identifying division boundaries for Hawai'i, as rainfall has notably greater variability compared to temperature.

b. Validation. The four statewide mean rainfall indices (GRID, STN-AVG, DIV-AVG, and DIV-WGT) show consistent monthly climatological evolution from January to December (Fig. 3a). The three indices GRID, DIV-AVG, and DIV-WGT show high consistency in both amplitude and seasonal evolution. The STN-AVG index is slightly higher than the other three, which could be caused by the inhomogeneous distribution of the rain gauge stations.

Figure 3b shows the year-to-year variability of annual rainfall amounts. The DIV-AVG index can faithfully represent the year-to-year variability of the GRID index (r = 0.99; Fig. 3b). The DIV-WGT index also resembles the GRID index (r = 0.86), with a bias that mainly occurs in the first 3 years. Therefore, partitioning the state into 12 divisions represents the statewide rainfall variability well.

Sensitivity tests were conducted using rainfall data from an earlier time period (1960–90; not shown). The results indicate that divisions established using data from 1960 to 1990 fail to distinguish between leeward and windward regions over Oahu and result in an additional division over Hawai'i Island. In contrast, insights from local experts suggest that the 12 divisions based on rainfall data during the period of 1990–2019 (Fig. 2a) exhibit physically meaningful divisions and are more robust and distinct.

c. Annual cycles. The peak rainfall months in Hawai'i are November, December, and March depending on the area of interest (Fig. 3a). Winter disturbances usually provide the majority of the precipitation for the drier leeward sides of the islands (Timm and Diaz 2009; Longman et al. 2021). The summer dry season, with June as the driest month on average (Fig. 3a), experiences persistent northeast trade winds, occasional tropical cyclones, and

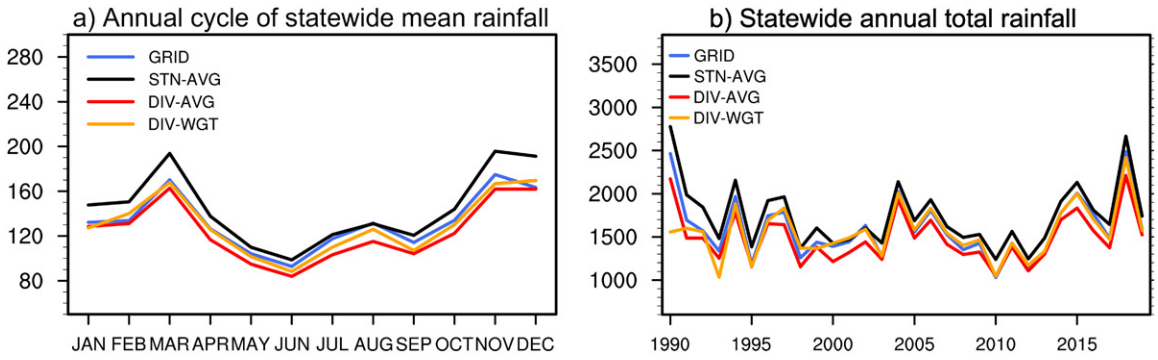

Fig. 3. Statewide mean rainfall validation of the 12 divisions. (a) Statewide rainfall seasonal cycle (mm month^{-1}) represented by four indices: the spatial average of the statewide gridded rainfall (GRID), the average of rainfall over all 618 stations (STN-AVG), the average of the stations within each of the 12 divisions and then an average of the 12 divisions (DIV-AVG), and the average of the stations within each of the 12 divisions and then an area-weighted average of the 12 divisions was calculated using the area of each division as the weight (DIV-WGT). (b) As in (a), but for the statewide mean annual rainfall time series during 1990–2019 (mm yr^{-1}).

few midlatitude rain-producing synoptic disturbances (Luo et al. 2020). Annual cycles of rainfall vary significantly across the state (Fig. 4). Divisions 5, 7, and 10 have the lowest average monthly values (<50 mm month^{-1}). Divisions 5 and 7 are located in the rain shadow areas of the tallest mountains in the state, Mauna Kea (4207 m) and Mauna Loa (4169 m) on Hawai'i Island, and Haleakalā (3055 m) on Maui. Hawai'i Mauka (division 10) receives low rainfall because of its high elevation location above the TWI, which caps cloud growth producing very dry, sunny area conditions (Longman et al. 2015). Divisions 1, 3, 9, and 11 have moderate monthly rainfall (between 50 and 100 mm month^{-1}), and they are mostly located in the leeward areas of the state. The windward divisions 2, 4, 6, and 8 have

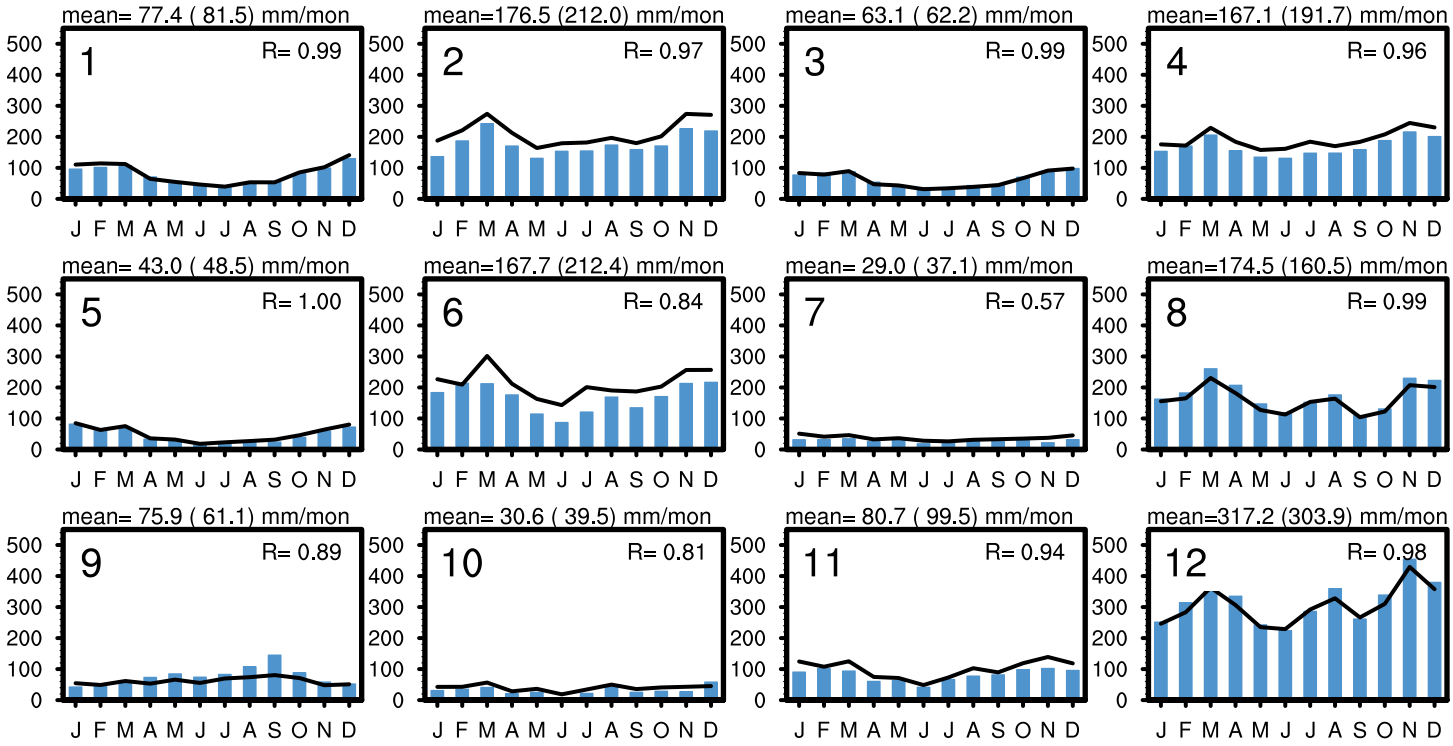

Fig. 4. Rainfall annual cycle averaged within each division (mm month^{-1}). Blue bars denote the average over all the rain gauge stations. Black lines are the rainfall average over all the grid points within each division. The annual mean rainfall based on station data is marked at the top of each panel (mm month^{-1}), and the numbers in parentheses are the annual mean average rainfall based on the gridded data. The *R* denotes the CC between the station data-derived and gridded data-derived annual cycles.

abundant rainfall with average monthly values ranging from 160 to 215 mm month^{-1}. The maximum rainfall rate of the state is found in the Hilo Division (12), with a precipitation rate of over 300 mm month^{-1}.

The seasonal cycles of rainfall show that most of the divisions have two or three peaks. Most of the divisions have peaks in March and November as frequent disturbances in these months bring intense rainfall across the state (Kodama and Businger 1998; Giambelluca et al. 2013; Longman et al. 2021). Meanwhile, some divisions, for example, divisions 6, 8, 10, 11, and 12, have a third monthly rainfall peak in August. The summer peak is likely related to a higher frequency of tropical cyclones (TCs). These TCs bring high winds and intense rainfall when they pass near the state (Nugent et al. 2020). Since these TCs originate in the eastern Pacific and have a westward-moving track, the affected areas are mostly over the southeastern part of the state, i.e., Hawai'i Island and Maui.

Most divisions have the same general seasonality as the statewide mean, i.e., a wet winter and a drier summer (Fig. 3). Kona is the only division with more rainfall in the summer months (Meisner 1976; Giambelluca et al. 1986, 2013; Kidd and McGregor 2007). This is because the winds flow around the Mauna Loa and, with thermal enhancement during the day, the orographic lifting of the local westerly flow produces persistent rainfall. This phenomenon is stronger during the summer, which gives the area a unique seasonality (Giambelluca et al. 1986; Chen and Nash 1994; Yang and Chen 2003; Huang and Chen 2019). The two seasonality indices (SI and R_{hl}) are shown in Fig. 5. A higher value of R_{hl} corresponds to stronger seasonality (greater range between the wettest and driest months). The results suggest that the Leeward Kaua'i, Waianae, and Leeward Maui Nui (divisions 1, 3, 5) have the greatest seasonality. For example, Leeward Kaua'i has 129.6 mm of rainfall in December, while it only has 38.5 mm of rainfall in July. Leeward Maui Nui has 81.7 mm of rainfall in January, in contrast with only 13.5 mm of rainfall in June. As indicated by SI, Leeward Maui Nui (division 5) is also rather seasonal with a short dry season. In contrast, Leeward Kaua'i, Waianae, and Ka'u (divisions 1, 3, 11) distinctly experience a wetter season. Other divisions have more uniform rainfall throughout the year.

d. Interannual and decadal rainfall variability. The scaled annual mean rainfall indices show clear decadal oscillations in most of the divisions (Fig. 6), indicating the potential

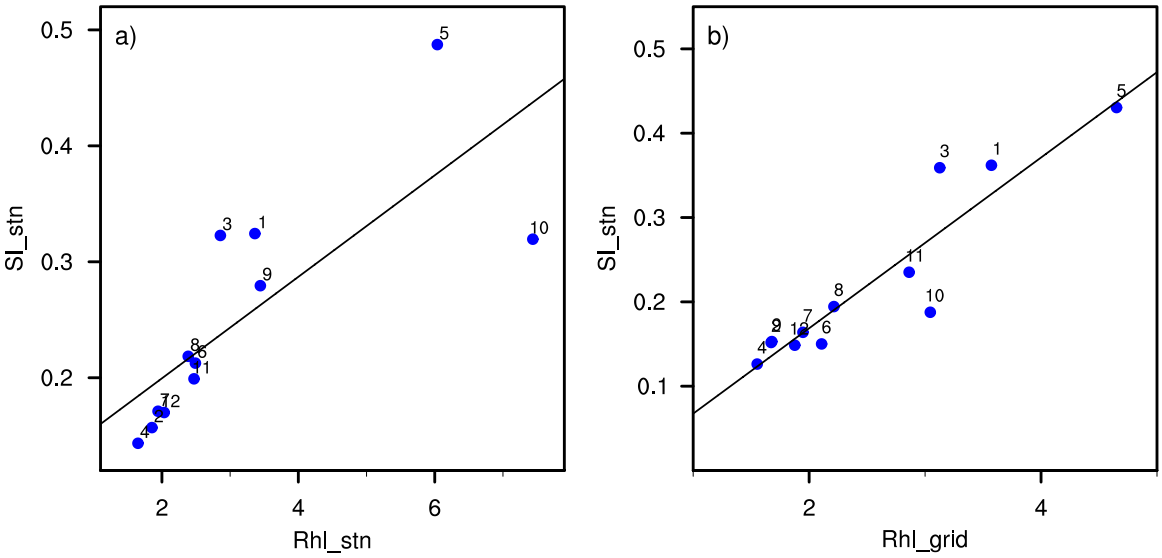

FIG. 5. Scatterplot of the seasonality strength of rainfall in each division (1–12) based on two seasonality indices: SI (*y* axis) vs R_{hl} (*x* axis). (a) SI vs R_{hl} derived from station rainfall data. (b) As in (a), but for gridded rainfall data. The division number associated with each blue point is labeled. The solid line denotes linear regression.

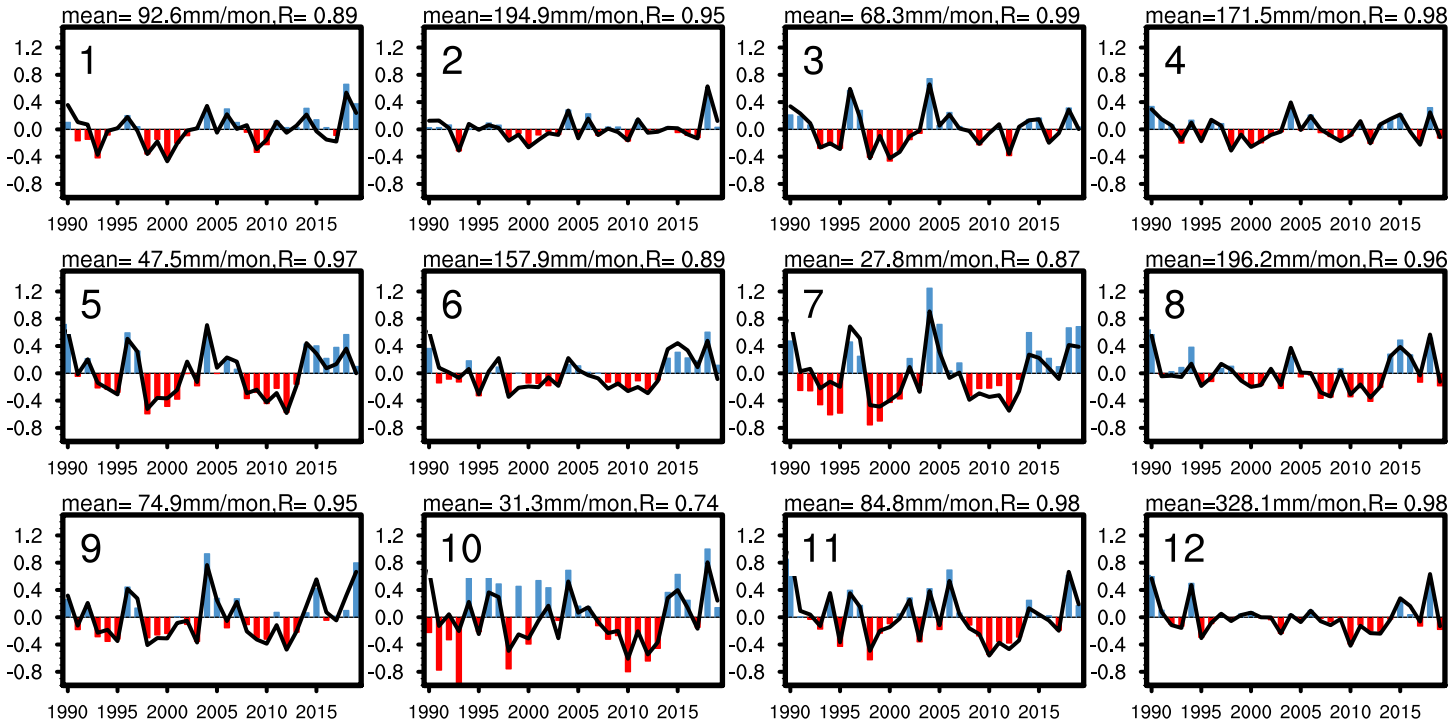

Fig. 6. Scaled anomalies of annual rainfall during 1990–2019 within each division. Scaled anomalies are calculated by dividing the annual rainfall anomalies by the climatological annual rainfall. Bars denote the average of all rain gauge stations within each division. Black lines are the rainfall average over all the grid points within each division. The long-term mean rainfall based on station data is marked at the top of each panel (mm month^{-1}). The *R* denotes the CC of the station data-derived and gridded data-derived rainfall time series.

impacts from ENSO variability (Diaz and Giambelluca 2012; Frazier et al. 2018). These are especially prominent for divisions 5–12, located in the southern half of the state. Two wet periods are notable after 1990: one during 2004/05 and a more recent wet period from 2014 to 2019. It is interesting to note that divisions 5–12 (Maui Nui and Hawai'i Island) have a consistent transition from a dry to a wet period around 2014 (Fig. 6). Three major dry periods have occurred during the recent 3 decades. The first one was 1993–95, significant in most of the drier leeward areas, i.e., divisions 1, 3, 5, 7, and 9 (Fig. 4), although it was not apparent in the statewide mean index (Fig. 3b). The second dry period occurred from 1998 to 2001 for 11 of the 12 divisions; it was not significant over windward Hawai'i Island (division 12). The third drought period spanned 2008–13 and was more prominent for Maui Nui and Hawai'i Island.

Hawai'i's climate is generally considered to have two 6-month seasons, a wet season (November–April) and a dry season (May–October), with the exceptions of windward areas which do not have a strong annual rainfall cycle, and the Kona region of Hawai'i Island which is has a summer rainfall maximum (Giambelluca et al. 2013). Because the wet season and dry season have different leading mechanisms for precipitation, it is of interest to diagnose whether the droughts in the annual mean analysis are contributed by anomalous wet season or dry season precipitation. The drought in 1993–95 was caused by a lack of rainfall in the wet season, and for most of the divisions, the drought started in 1991 (Fig. S1 in the online supplemental material). On the other hand, the dry season generally had above-average rainfall during these years (Fig. S2), though some discrepancies between the gridded and station values are apparent for divisions 7 and 10. The drought period in the years 1998–2001 was clear in both wet and dry seasons, which caused a stronger intensity and longer duration compared with the 1993–95 drought. The third drought was the most severe, and the signal was clear statewide for both seasons. These two droughts (1998–2002 and 2007–14) have

been identified as the worst droughts in the last century (Eischeid et al. 2022; Frazier et al. 2022), causing severe impacts across multiple sectors (Frazier et al. 2019). The downward trend in rainfall has been shown elsewhere to be part of a longer secular trend (Diaz et al. 2016; Frazier and Giambelluca 2017). Diaz and Giambelluca (2012) showed what appeared to be a decline in the strength of the correlation between the PDO and the winter season rainfall in Hawai'i. Eischeid et al. (2022) further considered this decline in the strength of that association, which favors wetter conditions during its cold (La Niña–like) phase over the past few decades. They concluded that the associative decline was likely mostly due to internal variability.

e. A century of rainfall variability, 1920–2019. Over the past century (1920–2019), monthly rainfall has exhibited decreasing trends in most of the divisions (Fig. 7a). These drying trends are particularly severe in divisions 7 and 9–11 on the western side of Hawai'i Island, ranging from −2.5% to −5.0% per decade (statistically significant at the 99% confidence level). The drying trends in divisions 2, 4, and 6 on the windward side of Kaua'i, O'ahu, and Maui Nui are also significant at the 95% confidence level. The scaled anomalies (Fig. 7b) show clear interannual and interdecadal variabilities, and a transition around the early 1980s from a wet phase to a 40-yr dry phase is notable in the southwest region of Hawai'i Island (divisions 9–11).

Table 2 lists the correlation coefficients between the ONI, PDO Index, and winter and summer rainfall during 1920–2019. During the wet season, both ENSO and PDO are negatively correlated with rainfall in all 12 divisions. Among the 12 divisions, rainfall over Kaua'i and southwest Hawai'i Island has the highest winter correlations with ENSO. Positive correlations are found between dry season rainfall and the ONI. The divisions on Maui and Hawai'i Islands (5–12, excluding 9) exhibit high dry season correlations. These results are consistent with previous studies (e.g., Frazier et al. 2018), as these regions are located within the southern flank of the western North Pacific cyclone and anticyclone anomalies and therefore tend to be modulated by the quasi-biennial component of ENSO (Luo et al. 2020). Summer rainfall has a higher correlation with PDO than winter rainfall, and the correlation in winter is not significant (Table 2).

Figure 8 illustrates the 31-yr running correlation coefficients (CCs) between the ONI during the ENSO mature phase (October to the following February) and divisional precipitation indices for both the wet season and dry season. The analysis covers three major affected divisions during the wet season and four major affected divisions during the dry season in Hawai'i. Significant multidecadal fluctuations are observed in the relationship between ENSO and divisional rainfall over Hawai'i. Before 1990, the relationship between ENSO and wet season divisional rainfall in Hawai'i was robust ($r < -0.5$). However, after 1990, this relationship has notably weakened over the three divisions. In the dry season, there was a weakening in the positive rainfall–ENSO relationship over Hilo and Windward divisions during the 1950s and 1960s and was gradually enhanced afterward.

f. Year-to-year temperature variability. We further show the annual mean temperature and its scaled anomaly in each division during 1990–2018 (Fig. 9). The highest annual mean temperature occurs in Leeward O'ahu (Waianae, division 3; 23.4°C), and unsurprisingly, the coldest division is Hawai'i Mauka (division 10; 10.8°C), which contains the highest elevation locations in the state (Fig. 1; see Giambelluca et al. 2014). The mean annual temperature has been increasing across the state. Most of the divisions have experienced two particularly warm episodes, i.e., 2000–06 and 2013–18. Before 2000, the state experienced relatively cooler temperatures (see also, McKenzie et al. 2019; Kagawa-Viviani and Giambelluca 2020).

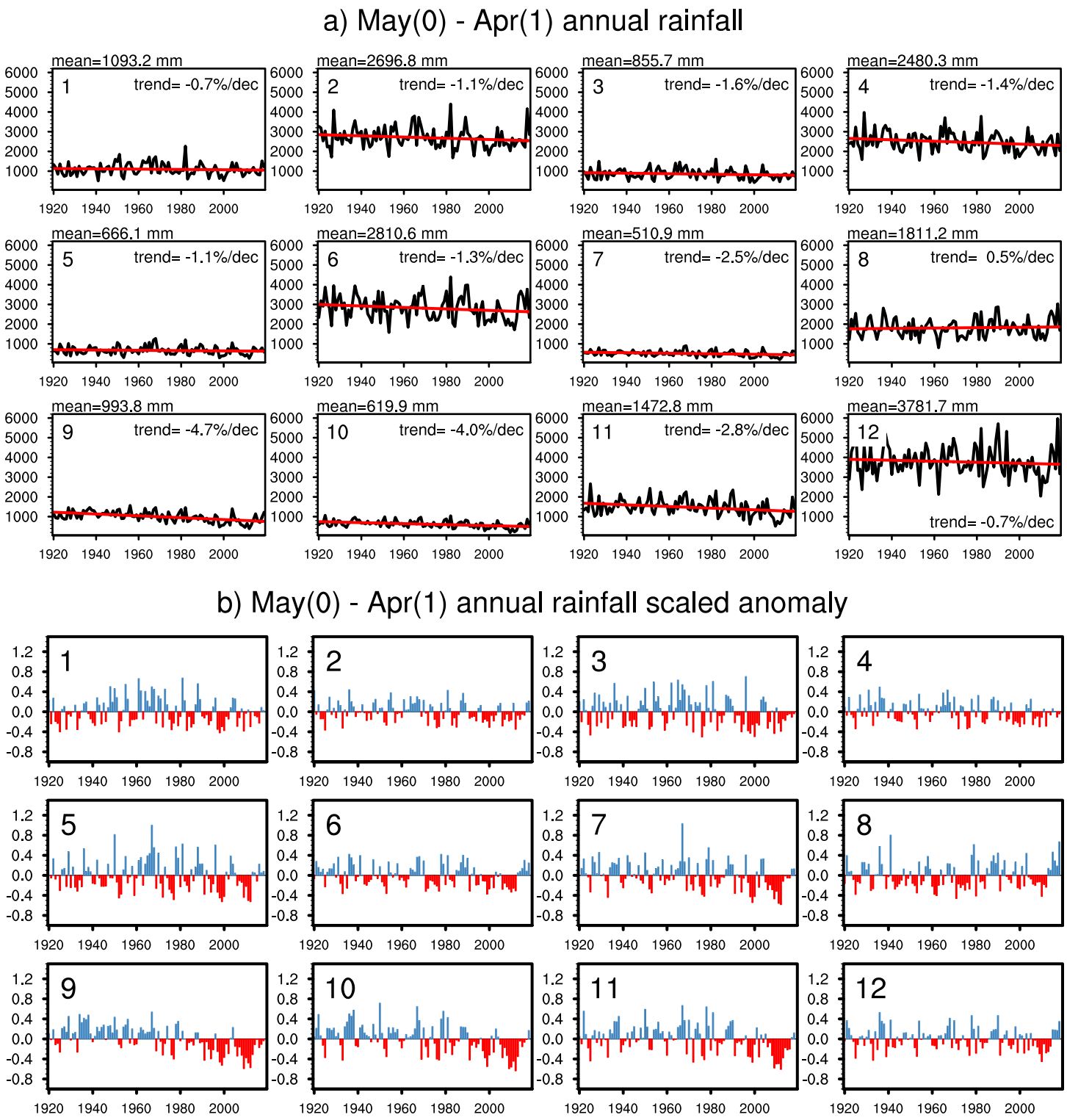

Fig. 7. Time series of the mean annual rainfall time series during 1920–2019 within each division. (a) The original grid-average rainfall time series (black line) with the respective linear trend (red line). The long-term mean rainfall is marked at the top of each panel (mm yr^{-1}). (b) Scaled anomalies of the annual rainfall, where the year is calculated from May to the following April to include the full wet season.

g. Research to operations. The division boundaries identified in this study are currently being integrated into NOAA NCEI's operations. Gridded 250-m climate data products from the Hawai'i Climate Data Portal (HCDP; Longman et al. 2024) will be used by the NCEI team, rather than adopting the 5-km gridding approach used for the CONUS (i.e., Vose et al. 2014). Climate records in Hawai'i are collected from stations in numerous networks, many of which are not part of national networks (Longman et al. 2018). By using HCDP products, NCEI will

TABLE 2. CCs between wet season (November–April) and dry season (May–October) rainfall (RF) with ONI and the annual PDO index from 1920 to 2019. Asterisks indicate that the CCs are statistically significant above the 95% confidence level considering the reduced degree of freedom.

Division number	*R* (ONI, wet season RF)	*R* (ONI, dry season RF)	*R* (PDO, wet season RF)	*R* (PDO, dry season RF)
1	−0.51*	0.38*	−0.41*	0.24*
2	−0.50*	0.30*	−0.35*	0.38*
3	−0.38*	0.32*	−0.25*	0.35*
4	−0.42*	0.25*	−0.23*	0.42*
5	−0.37*	0.42*	−0.14	0.45*
6	−0.25*	0.35*	0.01	0.49*
7	−0.34*	0.32*	−0.10	0.48*
8	−0.08	0.42*	0.12	0.45*
9	−0.45*	0.15	−0.20	0.39*
10	−0.44*	0.35*	−0.21	0.52*
11	−0.51*	0.47*	−0.31*	0.50*
12	−0.39*	0.43*	−0.24*	0.42*

be utilizing the most comprehensive dataset in the state. The incorporation of these data will allow NCEI to develop Hawai'i-specific products that currently do not exist.

While the indices derived from climate divisions in the CONUS use the period 1895 to the present and Alaska uses 1925 to the present, the Hawai'i gridded rainfall dataset is currently available from 1920 (with a smaller network of stations operating from 1837 to 1919; Frazier et al. 2016). The gridded temperature data are only available from 1990 onward due to the small station network and poor spatial coverage prior to 1990 (McKenzie et al. 2019; Kodama et al. 2024), which is an issue that may prompt the inclusion of the available long-term station data in some divisions to analyze long-term trends.

4. Conclusions

This study has established 12 official climate divisions for the state of Hawai'i based on an objective statistical method and local expert knowledge. The new climate divisions are essential to allow Hawai'i to have access to the historical climate analysis operational products from NOAA. The *k*-means cluster analysis has been applied to identify regions of homogeneous variability using the monthly gridded rainfall from 1990 to 2019. We determined that a total of 12 divisions effectively encapsulate the profound continental-scale spatial diversity in climate variability across the state while ensuring that the rainfall variability within each

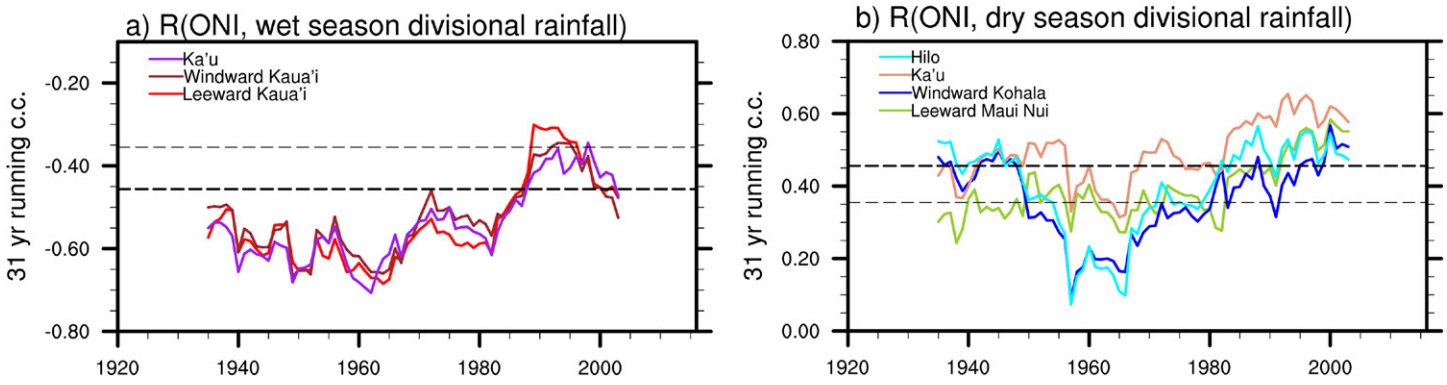

FIG. 8. The 31-yr running CCs between ONI from October to the next February and (a) wet season precipitation indices in three divisions (Leeward Kaua'i, Windward Kaua'i, and Ka'u) and (b) dry season precipitation indices in four divisions (Hilo, Ka'u, Windward Kohala, and Leeward Maui Nui). Thick (thin) dashed lines indicate the 99% (95%) significance level for a 31-yr running CC.

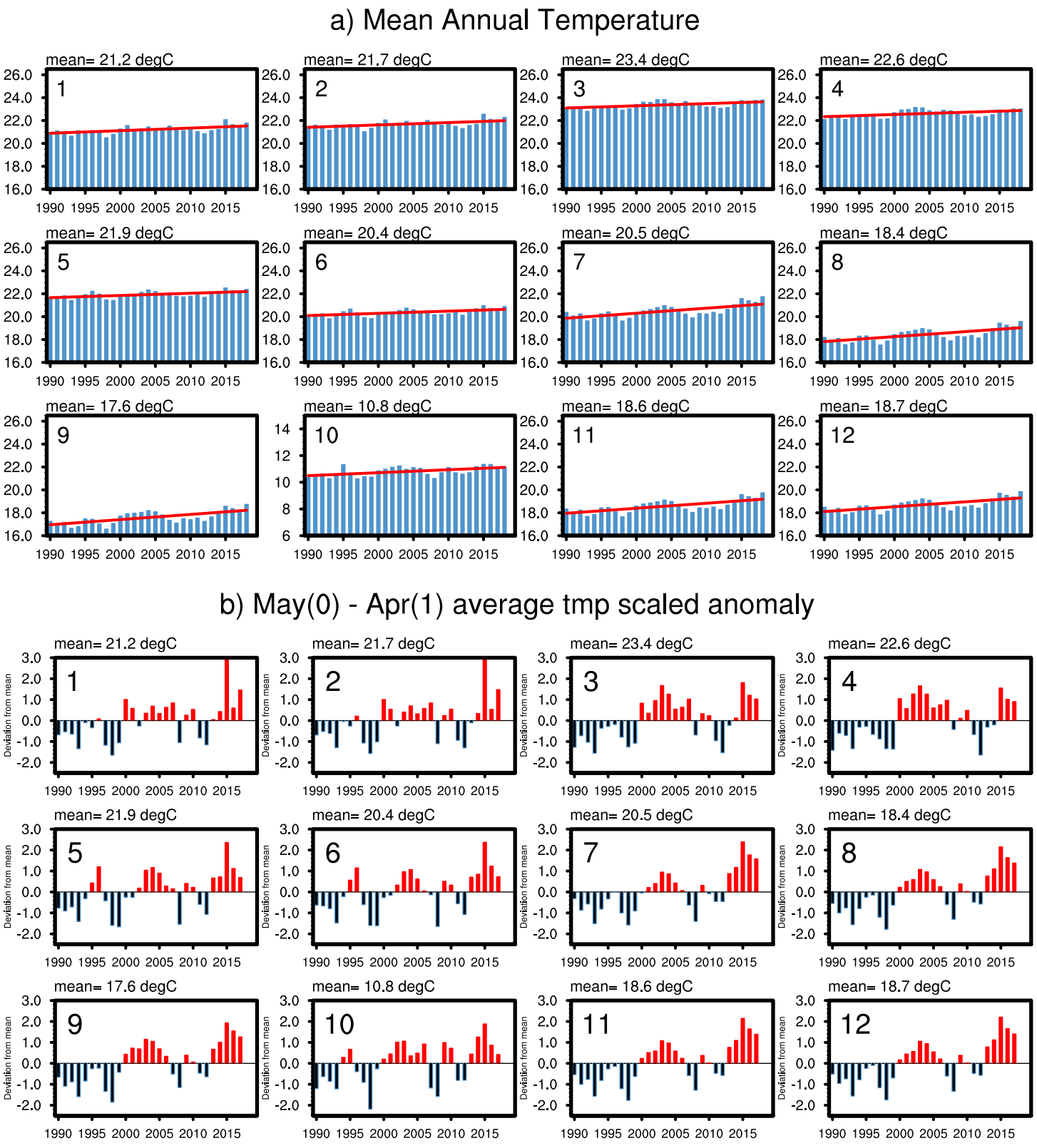

FIG. 9. Mean annual temperature during 1990–2018 within each division. (a) The original mean temperature time series (°C) with the respective linear trends (red line). (b) The scaled anomalies of mean annual temperature, where the year is calculated from May to the following April. Scaled temperature anomalies are calculated by dividing the temperature anomalies by their standard deviations. All graphs are shown on consistent axes within the respective panel except in the top panel, where the coldest division 10 is shown on a different *y*-axis scale.

division remained independent from the others. With the new climate divisions, we find that the DIV-WGT rainfall index varies consistently with the GRID statewide average rainfall index, except for the minor bias during 1990–92 (Fig. 3b). Therefore, these climate divisions can be applied to station rainfall to provide real-time monitoring for the state.

The annual cycle analysis shows that most of the divisions have two or three peaks in their climatological seasonal evolution of rainfall. The frequent occurrence of disturbances in November and March (Longman et al. 2021) explains two peaks for most of the climate divisions. In some windward divisions in the southern part of the state, TCs are more frequent and can cause extreme rainfall when they pass across the state or in the vicinity of an island (e.g., Nugent et al. 2020), thus likely causing a third peak in their annual rainfall in August. The Kona Division has more rainfall in the summer months, in contrast with all the other divisions in Hawai'i. The seasonality ratios suggest that the Leeward Kaua'i, Leeward Maui Nui, and Hawai'i Mauka Divisions have the strongest seasonality.

The annual rainfall indices show that there were two strong dry periods during the recent 3 decades. One was from 1998 to 2001 and was widespread but not significant over the windward part of Hawai'i Island (division 12). Another drought period spanned 2008–13 with a clear signal over the southern part of the state, i.e., excluding Kaua'i and O'ahu. Both the wet and dry seasons show clear interannual and decadal rainfall variations. In the wet season, most of the southern part of Hawai'i Island had a long-lasting dry period during 2009–15. After 2017, most of the state started to enter a wetter period. In the dry season, most of the state received deficient rainfall for nearly 2 decades beginning in 1994, with a striking transition to a wetter period in 2014. This signal is also stronger in the southern part of Hawai'i. Long-term decreasing trends in annual rainfall during the recent 100 years are most significant on the western side of Hawai'i Island, ranging between –2.5% and –5.0% per decade, coinciding with a transition from wet to dry phase around the early 1980s.

The division boundaries identified in this study and corresponding new access to NOAA products for Hawai'i will promote future research on climate forecasting and improve climate change decision-making across the state. This work will support the development of new monitoring efforts, including the Hawai'i mesoscale meteorological network (Mesonet; Giambelluca et al. 2024), and fills a critically important gap in NOAA's national coverage, moving toward better data equity and coverage outside the CONUS. This project is an important step toward improving climate resilience and creating true "national" products that include every part of the United States.

Acknowledgments. This research was funded by NOAA Award NA21NWS4680001. The authors thank J. Marra and R. Vose from NOAA for their support on this project and K. Kodama, D. Simeral, and P. S.-Chu for early discussions about this effort.

Data availability statement. The climate division GIS layer results are available for download from https://github.com/abbyfrazier/HIClimateDivisions.

References

Adhikari, M., R. J. Longman, T. W. Giambelluca, C. N. Lee, and Y. He, 2022: Climate change impacts shifting landscape of the dairy industry in Hawai'i. *Transl. Anim. Sci.*, **6**, txac064, https://doi.org/10.1093/tas/txac064.

Barbosa, J. M., and G. P. Asner, 2017: Effects of long-term rainfall decline on the structure and functioning of Hawaiian forests. *Environ. Res. Lett.*, **12**, 094002, https://doi.org/10.1088/1748-9326/aa7ee4.

Basile, S., C. W. Avery, A. Grade, and A. R. Crimmins, 2024: To be policy-relevant, future climate research must include the noncontiguous United States. *Proc. Natl. Acad. Sci*., **121**, e2315505121, https://doi.org/10.1073/pnas.2315505121.

Bieniek, P. A., and Coauthors, 2012: Climate divisions for Alaska based on objective methods. *J. Appl. Meteor. Climatol.*, **51**, 1276–1289, https://doi.org/10.1175/JAMC-D-11-0168.1.

Chen, Y.-L., and A. J. Nash, 1994: Diurnal variation of surface airflow and rainfall frequencies on the island of Hawaii. *Mon. Wea. Rev.*, **122**, 34–56, https://doi.org/10.1175/1520-0493(1994)122<0034:DVOSAA>2.0.CO;2.

Chu, P.-S., and H. Chen, 2005: Interannual and interdecadal rainfall variations in the Hawaiian Islands. *J. Climate*, **18**, 4796–4813, https://doi.org/10.1175/JCLI3578.1.

Clilverd, H. M., Y.-P. Tsang, D. M. Infante, A. J. Lynch, and A. M. Strauch, 2019: Long-term streamflow trends in Hawai'i and implications for native stream fauna. *Hydrol. Processes*, **33**, 699–719, https://doi.org/10.1002/hyp.13356.

Corrigan, T. J., Jr., and S. Businger, 2022: The anatomy of a series of cloud bursts that eclipsed the U.S. rainfall record. *Mon. Wea. Rev.*, **150**, 753–773, https://doi.org/10.1175/MWR-D-21-0028.1.

Diaz, H. F., and T. W. Giambelluca, 2012: Changes in atmospheric circulation patterns associated with high and low rainfall regimes in the Hawaiian Islands region on multiple time scales. *Global Planet. Change*, **98–99**, 97–108, https://doi.org/10.1016/j.gloplacha.2012.08.011.

——, E. R. Wahl, E. Zorita, T. W. Giambelluca, and J. K. Eischeid, 2016: A five-century reconstruction of Hawaiian Islands rainfall. *J. Climate*, **29**, 5661–5674, https://doi.org/10.1175/JCLI-D-15-0815.1.

Durre, I., A. Arguez, C. J. Schreck III, M. F. Squires, and R. S. Vose, 2022: Daily high-resolution temperature and precipitation fields for the contiguous United States from 1951 to present. *J. Atmos. Oceanic Technol.*, **39**, 1837–1855, https://doi.org/10.1175/JTECH-D-22-0024.1.

Eischeid, J. K., M. P. Hoerling, X.-W. Quan, and H. F. Diaz, 2022: Diagnosing Hawaii's recent drought. *J. Climate*, **35**, 3997–4012, https://doi.org/10.1175/JCLI-D-21-0754.1.

Frauendorf, T. C., R. A. MacKenzie, R. W. Tingley III, A. G. Frazier, M. H. Riney, and R. W. El-Sabaawi, 2019: Evaluating ecosystem effects of climate change on tropical island streams using high spatial and temporal resolution sampling regimes. *Global Change Biol.*, **25**, 1344–1357, https://doi.org/10.1111/gcb.14584.

Frazier, A. G., and T. W. Giambelluca, 2017: Spatial trend analysis of Hawaiian rainfall from 1920 to 2012. *Int. J. Climatol.*, **37**, 2522–2531, https://doi.org/10.1002/joc.4862.

——, ——, H. F. Diaz, and H. L. Needham, 2016: Comparison of geostatistical approaches to spatially interpolate month-year rainfall for the Hawaiian Islands. *Int. J. Climatol.*, **36**, 1459–1470, https://doi.org/10.1002/joc.4437.

——, O. Elison Timm, T. W. Giambelluca, and H. F. Diaz, 2018: The influence of ENSO, PDO and PNA on secular rainfall variations in Hawai'i. *Climate Dyn.*, **51**, 2127–2140, https://doi.org/10.1007/s00382-017-4003-4.

——, and Coauthors, 2019: Managing effects of drought in Hawai'i and U.S.-affiliated Pacific Islands. U.S. Department of Agriculture, Forest Service, Washington Office, General Tech. Rep. WO-98, 95–121, https://www.fs.usda.gov/research/treesearch/59164.

——, and Coauthors, 2022: A century of drought in Hawai'i: Geospatial analysis and synthesis across hydrological, ecological, and socioeconomic scales. *Sustainability*, **14**, 12023, https://doi.org/10.3390/su141912023.

——, and Coauthors, 2023: Hawai'i and US-Affiliated Pacific Islands. *Fifth National Climate Assessment*, A. R. Crimmins et al., Eds., U.S. Global Change Research Program, https://doi.org/10.7930/NCA5.2023.CH30.

Getz, D., and P. A. Nilsson, 2004: Responses of family businesses to extreme seasonality in demand. *Tourism Manage.*, **25**, 17–30, https://doi.org/10.1016/S0261-5177(03)00067-0.

Giambelluca, T. W., M. A. Nullet, and T. A. Schroeder, 1986: Rainfall Atlas of Hawaii. Department of Land and Natural Resources Rep. R76, 267 pp.

——, Q. Chen, A. G. Frazier, J. P. Price, Y.-L. Chen, P.-S. Chu, J. K. Eischeid, and D. M. Delparte, 2013: Online rainfall atlas of Hawai'i. *Bull. Amer. Meteor. Soc.*, **94**, 313–316, https://doi.org/10.1175/BAMS-D-11-00228.1.

——, and Coauthors, 2014: Evapotranspiration of Hawai'i. U.S. Army Corps of Engineers—Honolulu District, and the Commission on Water Resource Management, State of Hawai'i Final Rep., 178 pp., http://evapotranspiration.geography.hawaii.edu/assets/files/PDF/ET%20Project%20Final%20Report.pdf.

——, and Coauthors, 2024: The Hawai'i Mesonet: A 100-station real-time weather and climate monitoring network across Hawai'i's steep gradients. *28th Conf. on Applied Climatology*, Baltimore, MD, Amer. Meteor. Soc., 7.5, https://ams.confex.com/ams/104ANNUAL/meetingapp.cgi/Paper/436763.

Guttman, N. B., and R. G. Quayle, 1996: A historical perspective of U.S. climate divisions. *Bull. Amer. Meteor. Soc.*, **77**, 293–304, https://doi.org/10.1175/1520-0477(1996)077<0293:AHPOUC>2.0.CO;2.

Huang, B., and Coauthors, 2017: Extended Reconstructed Sea Surface Temperature, version 5 (ERSSTv5): Upgrades, validations, and intercomparisons. *J. Climate*, **30**, 8179–8205, https://doi.org/10.1175/JCLI-D-16-0836.1.

Huang, Y.-F., and Y.-L. Chen, 2019: Numerical simulations of seasonal variations of rainfall over the Island of Hawaii. *J. Appl. Meteor. Climatol.*, **58**, 1219–1232, https://doi.org/10.1175/JAMC-D-18-0078.1.

Kagawa-Viviani, A. K., and T. W. Giambelluca, 2020: Spatial patterns and trends in surface air temperatures and implied changes in atmospheric moisture across the Hawaiian Islands, 1905–2017. *J. Geophys. Res. Atmos.*, **125**, e2019JD031571, https://doi.org/10.1029/2019JD031571.

Keener, V., and Coauthors, 2018: Hawai'i and U.S.-Affiliated Pacific Islands. *Impacts, Risks, and Adaptation in the United States: Fourth National Climate Assessment, Volume II*, D. R. Reidmiller et al., Eds., U.S. Global Change Research Program, 1242–1308, https://doi.org/10.7930/NCA4.2018.CH27.

Keener, V. W., Z. N. Grecni, and S. C. Moser, 2022: Accelerating climate change adaptive capacity through regional sustained assessment and evaluation in Hawai'i and the U.S. Affiliated Pacific Islands. *Front. Climate*, **4**, 869760, https://doi.org/10.3389/fclim.2022.869760.

Kidd, C., and G. McGregor, 2007: Observation and characterisation of rainfall over Hawaii and surrounding region from the Tropical Rainfall Measuring Mission. *Int. J. Climatol.*, **27**, 541–553, https://doi.org/10.1002/joc.1414.

Kodama, K. M., and Coauthors, 2024: Mapping daily air temperature over the Hawaiian Islands from 1990 to 2021 via an optimized piecewise linear regression technique. *Earth Space Sci.*, **11**, e2023EA002851, https://doi.org/10.1029/2023EA002851.

Kodama, K. R., and S. Businger, 1998: Weather and forecasting challenges in the Pacific region of the National Weather Service. *Wea. Forecasting*, **13**, 523–546, https://doi.org/10.1175/1520-0434(1998)013<0523:WAFCIT>2.0.CO;2.

Longman, R. J., H. F. Diaz, and T. W. Giambelluca, 2015: Sustained increases in lower-tropospheric subsidence over the central tropical North Pacific drive a decline in high-elevation rainfall in Hawaii. *J. Climate*, **28**, 8743–8759, https://doi.org/10.1175/JCLI-D-15-0006.1.

——, and Coauthors, 2018: Compilation of climate data from heterogeneous networks across the Hawaiian Islands. *Sci. Data*, **5**, 180012, https://doi.org/10.1038/sdata.2018.12.

——, and Coauthors, 2019: High-resolution gridded daily rainfall and temperature for the Hawaiian Islands (1990–2014). *J. Hydrometeor.*, **20**, 489–508, https://doi.org/10.1175/JHM-D-18-0112.1.

——, A. J. Newman, T. W. Giambelluca, and M. Lucas, 2020: Characterizing the uncertainty and assessing the value of gap-filled daily rainfall data in Hawaii. *J. Appl. Meteor. Climatol.*, **59**, 1261–1276, https://doi.org/10.1175/JAMC-D-20-0007.1.

——, O. E. Timm, T. W. Giambelluca, and L. Kaiser, 2021: A 20-year analysis of disturbance-driven rainfall on O'ahu, Hawai'i. *Mon. Wea. Rev.*, **149**, 1767–1783, https://doi.org/10.1175/MWR-D-20-0287.1.

——, and Coauthors, 2024: The Hawai'i Climate Data Portal (HCDP). *Bull. Amer. Meteor. Soc.*, https://doi.org/10.1175/BAMS-D-23-0188.1.

Lucas, M. P., C. Trauernicht, A. G. Frazier, and T. Miura, 2020: Long-term, gridded standardized precipitation index for Hawai'i. *Data*, 2020, **5**, 109, https://doi.org/10.3390/data5040109.

——, R. J. Longman, T. W. Giambelluca, A. G. Frazier, J. Mclean, S. B. Cleveland, Y.-F. Huang, and J. Lee, 2022: Optimizing automated kriging to improve spatial interpolation of monthly rainfall over complex terrain. *J. Hydrometeor.*, **23**, 561–572, https://doi.org/10.1175/JHM-D-21-0171.1.

Luo, X., B. Wang, A. G. Frazier, and T. W. Giambelluca, 2020: Distinguishing variability regimes of Hawaiian summer rainfall: Quasi-biennial and interdecadal oscillations. *Geophys. Res. Lett.*, **47**, e2020GL091260, https://doi.org/10.1029/2020GL091260.

Mantua, N. J., S. R. Hare, Y. Zhang, J. M. Wallace, and R. C. Francis, 1997: A Pacific interdecadal climate oscillation with impacts on salmon production. *Bull. Amer. Meteor. Soc.*, **78**, 1069–1080, https://doi.org/10.1175/1520-0477(1997)078<1069:APICOW>2.0.CO;2.

McKenzie, M. M., T. W. Giambelluca, and H. F. Diaz, 2019: Temperature trends in Hawai'i: A century of change, 1917–2016. *Int. J. Climatol.*, **39**, 3987–4001, https://doi.org/10.1002/joc.6053.

Meisner, B. N., 1976: A study of Hawaiian and Line Islands rainfall. M.S. thesis, Dept. of Meteorology, University of Hawaii at Manoa, 83 pp.

Méndez-Lazaro, P. A., and Coauthors, 2023: US Caribbean. *Fifth National Climate Assessment*, A. R. Crimmins et al., Eds., U.S. Global Change Research Program, 57 pp., https://doi.org/10.7930/NCA5.2023.CH23.

Nugent, A. D., R. J. Longman, C. Trauernicht, M. P. Lucas, H. F. Diaz, and T. W. Giambelluca, 2020: Fire and rain: The legacy of Hurricane Lane in Hawai'i. *Bull. Amer. Meteor. Soc.*, **101**, E954–E967, https://doi.org/10.1175/BAMS-D-19-0104.1.

Rayner, N. A., D. E. Parker, E. B. Horton, C. K. Folland, L. V. Alexander, D. P. Rowell, E. C. Kent, and A. Kaplan, 2003: Global analyses of sea surface temperature, sea ice, and night marine air temperature since the late nineteenth century. *J. Geophys. Res.*, **108**, 4407, https://doi.org/10.1029/2002JD002670.

Timm, O., and H. F. Diaz, 2009: Synoptic-statistical approach to regional downscaling of IPCC twenty-first-century climate projections: Seasonal rainfall over the Hawaiian Islands. *J. Climate*, **22**, 4261–4280, https://doi.org/10.1175/2009JCLI2833.1.

Vose, R. S., and Coauthors, 2014: Improved historical temperature and precipitation time series for U.S. climate divisions. *J. Appl. Meteor. Climatol.*, **53**, 1232–1251, https://doi.org/10.1175/JAMC-D-13-0248.1.

Walsh, R. P. D., and D. M. Lawler, 1981: Rainfall seasonality: Description, spatial patterns and change through time. *Weather*, **36**, 201–208, https://doi.org/10.1002/j.1477-8696.1981.tb05400.x.

Wilks, D. S., 2011: *Statistical Methods in the Atmospheric Sciences.* 3rd ed. Elsevier, 676 pp.

Yang, Y., and Y.-L. Chen, 2003: Circulations and rainfall on the leeside of the island of Hawaii during HaRP. *Mon. Wea. Rev.*, **131**, 2525–2542, https://doi.org/10.1175/1520-0493(2003)131<2525:CAROTL>2.0.CO;2.